High discharge energy density in novel K1/2Bi1/2TiO3-BiFeO3 based relaxor ferroelectrics

WANG, X., FAN, Y., ZHANG, Bin, MOSTAED, A., LI, L., FETEIRA, Antonio <http://orcid.org/0000-0001-8151-7009>, WANG, D., SINCLAIR, D.C., WANG, G. and REANEY, I.M.

Published version

WANG, X., FAN, Y., ZHANG, Bin, MOSTAED, A., LI, L., FETEIRA, Antonio, WANG, D., SINCLAIR, D.C., WANG, G. and REANEY, I.M. (2022). High discharge energy density in novel K1/2Bi1/2TiO3-BiFeO3 based relaxor ferroelectrics. Journal of the European Ceramic Society, 42 (15), 7381-7387.

Electronic Supplementary information (ESI)

High discharge energy density in novel $K_{1/2}Bi_{1/2}TiO_3$-$BiFeO_3$ based relaxor ferroelectrics

Xinzhen Wang,[a, b] Yongbo Fan,[a] Bin Zhang,[c] Ali Mostaed,[d] Linhao Li,[e] Antonio Feteira,[f] Dawei Wang,[c] Derek C. Sinclair,[a] Ge Wang[a,g*] and Ian M. Reaney[a*]

[a] Department of Materials Science and Engineering, University of Sheffield, Sheffield, S1 3JD, UK
[b] School of Materials Science and Engineering, Shandong University of Science and Technology, Qingdao, 266590, China
[c] Shenzhen Institute of Advanced Electronic Materials, Shenzhen Institute of Advanced Technology, Chinese Academy of Sciences, Shenzhen, 518055, China
[d] Department of Materials, University of Oxford, Oxford, OX1 3PH, UK
[e] School of Mathematics and Physics, Beijing University of Chemical Technology, Beijing, 100013, China
[f] Materials and Engineering Research Institute, Sheffield Hallam University, Sheffield, S1 1WB, UK
[g] Department of Materials, University of Manchester, Manchester, S13 9PL, UK

Table S1. Refined crystallographic information for the KBT-BT-xSMN ceramics

x	Lattice parameter/ Å	Volume / Å^3	GOF
0.00	3.95287(19)	61.764(9)	1.11
0.04	3.9550(3)	61.863(12)	1.05
0.08	3.95947(4)	62.0742(18)	1.09

Figure S1. BSE images obtained from polished surfaces of the KBT-BF-xSMN ceramics for (a) x=0.00, (b) x=0.02, (c) x=0.04, (d) x=0.06, (e) x=0.08 and (f) x=0.10 at the same magnification.

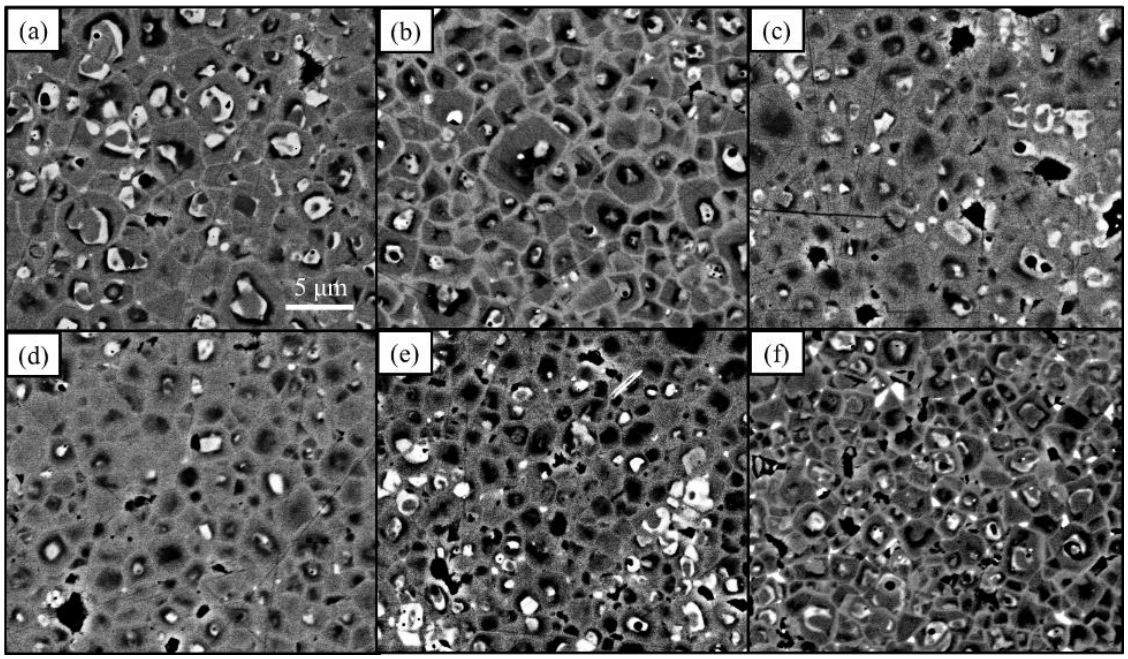

Figure S2. EDX elemental point analysis on a polished surface of the KBT-BF-0.08SMN ceramic.

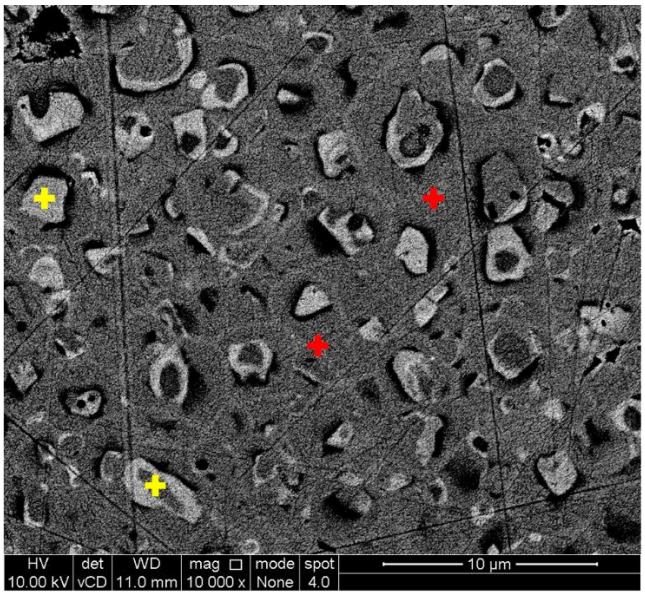

	Bi(at%)	Fe(at%)	K(at%)	Ti(at%)	
Core 1	23.7 ↑	19.1 ↑	3.1	5.8	Bi/Fe-rich
Core 2	23.6 ↑	18.5 ↑	3.2	6.4	
Shell 1	17.7	14.5	4.9 ↑	10.3 ↑	K/Ti-rich
Shell 2	17.8	15.1	5.5 ↑	11.0 ↑	

Table S2. Average grain size of the KBT-BF-xSMN ceramics.

Compositions x	Average grain size (μm)
0.00	2.95±0.56
0.02	2.58±0.44
0.04	2.25±0.40
0.06	2.20±0.35
0.08	2.14±0.28
0.10	2.31±0.17

Figure S3. Temperature-dependent permittivity and dielectric loss data of the KBT-BF-xSMN ceramics for (a) x=0.00, (b) x=0.02, (c) x=0.04, (d) x=0.06, (e) x=0.08 and (f) x=0.10 at frequencies of 10 kHz, 100 kHz, 250 kHz and 1 MHz.

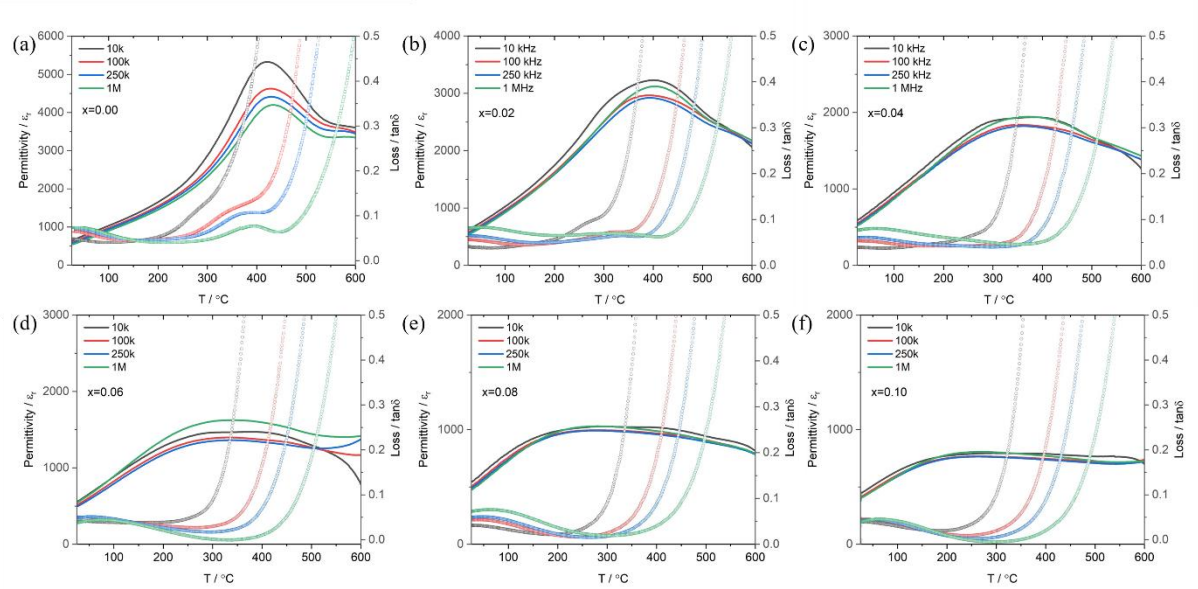

Figure S4. Unipolar P-E loops of the KBT-BF-xSMN bulk ceramics for (a) x=0.04, (b) x=0.06, (c) x=0.08 and (d) x=0.10.

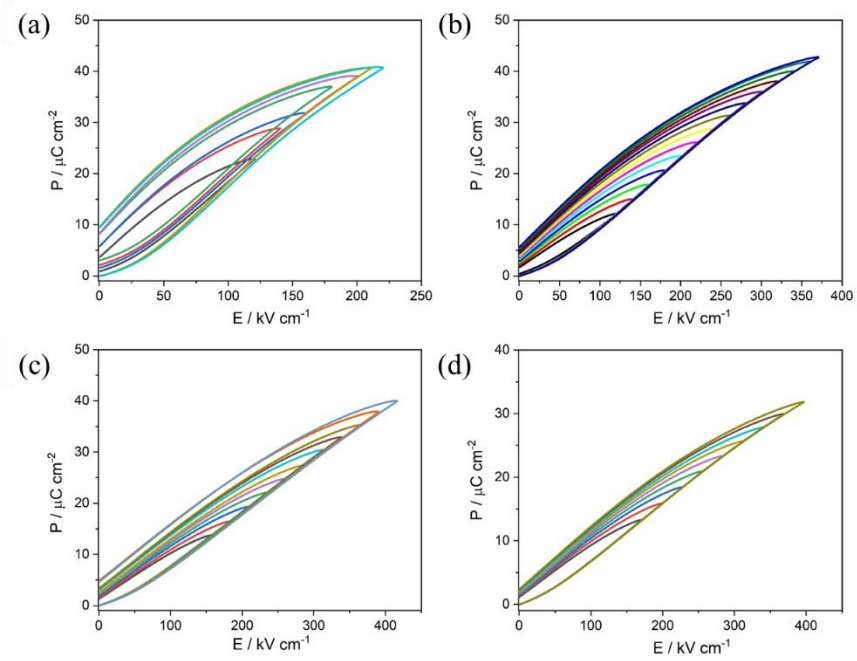

Figure S5. Calculated energy storage performance of the KBT-BF-xSMN ceramics for (a) x=0.04, (b) x=0.06, (c) x=0.08 and (d) x=0.10.

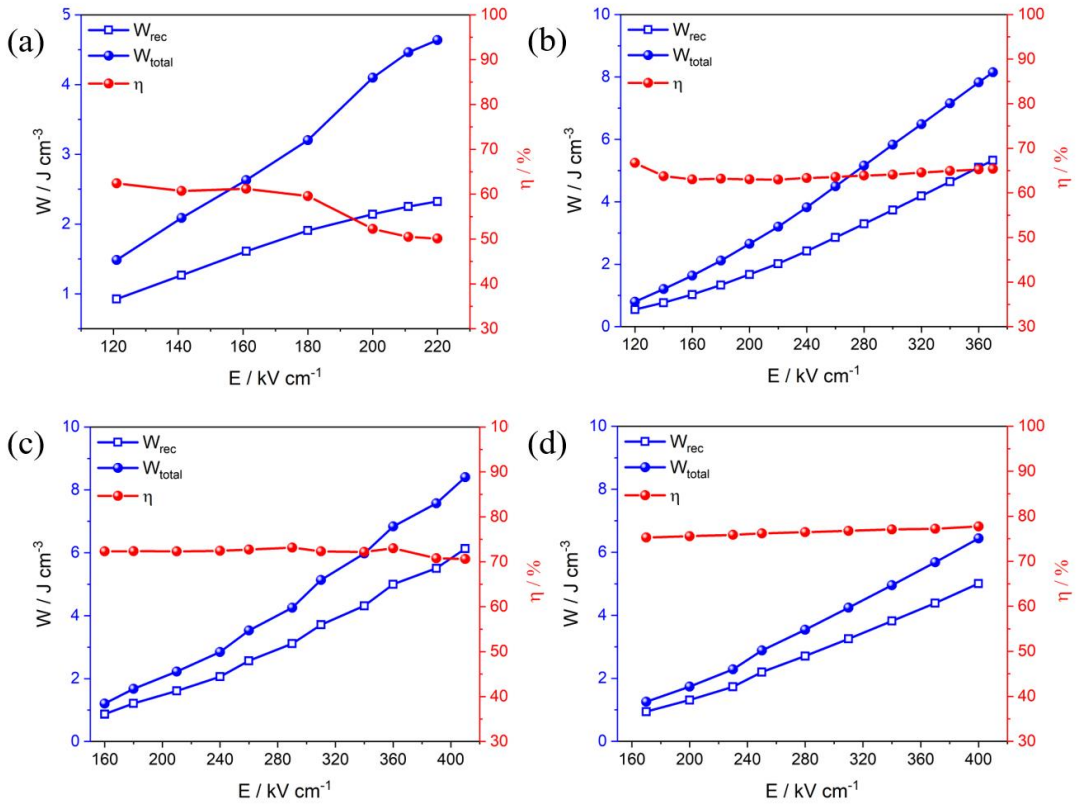

Figure S6. Complex Z* plots of the KBT-BF-xSMN ceramics x=0.00 and x=0.08 at 400°C.